

# Synergy of Homogeneous and Heterogeneous Chemistry Probed by In Situ Spatially Resolved Measurements of Temperature and Composition

Alessandro Donazzi, Dario Livio, Matteo Maestri, Alessandra Beretta,\* Gianpiero Groppi, Enrico Tronconi, and Pio Forzatti

The interaction between heterogeneous and homogeneous chemistries is a crucial issue for high-temperature catalytic processes. In particular, the assessment of the main routes that control the selectivity to the desired products is essential for the design and safe operation of reaction units. This assessment is particularly true for the ultrafast conversion of hydrocarbons in short-contact-time (SCT) reactors that play a pivotal role in the effort to cope with the worldwide growing demand for more efficient exploitation of energy and material resources. Examples are the catalytically assisted combustion for gas turbines with ultralow emissions, the catalytic partial oxidation (CPO) of hydrocarbons to  $H_2$  or  $CO/H_2$  mixtures (i.e., syngas),<sup>[1]</sup> and the oxidative dehydrogenation (ODH) of light alkanes to olefins.<sup>[2,3]</sup> As a common feature, these processes operate in autothermal and compact reactors, with noble-metal catalysts (palladium, rhodium, and platinum). An enormous energy intensity is peculiar to the SCT autothermal conversion of hydrocarbons over noble metals. Strongly exothermic and endothermic reactions proceed on the catalyst surface at extremely high rates. As a consequence, sharp gradients of temperature (up to  $200^\circ\text{Cmm}^{-1}$ ) and concentration are established within the small reactor volumes. Temperatures ranging from 250 to  $1100^\circ\text{C}$  are generally experienced within a few millimeters. Such a level of severity—in terms of power density and extent of temperature and concentration gradients—is typical of flames and gas-phase oxidation processes in general. For a catalytic process, however, these conditions represent a thoroughly unconventional kinetic regime. To best grasp the intensity and the speed of the involved phenomena, we need to think of SCT conversion of light alkanes as the catalytic equivalent of a flame. This analogy can clearly depict the complexity of the process and emphasize the related scientific issues: To what extent does a catalytic process “stick” to the catalyst surface at these very high temperatures, where the adsorption of species is thermodynamically unfavored? Can the gas-phase activation of C–H bonds (e.g., the formation and propagation of radicals) cooperate or compete with the catalytic process?

In this respect, it is largely accepted that in the case of  $CH_4$  CPO over rhodium the gas-phase paths are negligible at atmospheric pressure and the catalytic route dominates.<sup>[4–6]</sup> Conversely, the SCT-ODH of short alkanes over platinum proceeds mainly in the gas phase, thus giving rise to the production of olefins and other hydrocarbon species.<sup>[7,8]</sup> On the basis of these examples, we could conclude that either catalytic or gas-phase chemistry governs the SCT conversion of hydrocarbons, depending only on the stability of the C–H bond in the gas phase.

Herein, by using novel techniques for collecting spatially resolved temperature and concentration profiles, we show that the partial oxidation of short-chain alkanes over rhodium breaks the paradigmatic compartments of heterogeneous processes and gas-phase processes, revealing the real complexity of these “flame-like” processes.

Specifically, we examine the reaction of  $C_3H_8$  CPO ( $C_3H_8 + 3/2 O_2 \rightarrow 3 CO + 4 H_2$ ) as a case study, and we apply novel techniques for collecting spatially resolved gas-phase and solid temperature and concentration profiles within a rhodium-coated honeycomb monolith to monitor the evolution of a propane/air mixture fed at high flow rate. The temperature and the composition of the reacting system were monitored from the inlet reactor section where the mixture was fed to the outlet section of the catalytic unit where the syngas stream was delivered.

The results are reported in Figure 1 and Figure 2 as spatially resolved profiles of temperature and molar fraction of reactants and products. In the first 5 mm of the honeycomb, a sharp drop of  $O_2$  and  $C_3H_8$  concentration was observed, accompanied by the formation of total oxidation products ( $CO_2$  and  $H_2O$ ) and partial oxidation products ( $H_2$  and  $CO$ ). Correspondingly, a hot spot formed on the catalyst surface ( $980^\circ\text{C}$ , measured by the pyrometer) and a steep rise was observed in the gas temperature (up to  $945^\circ\text{C}$ , measured by the thermocouple). In line with the occurrence of the endothermic steam reforming reaction, the evolution of  $H_2O$  showed a maximum. Moreover, the temperature of the solid surface and in the gas phase decreased toward the exit of the honeycomb. Qualitatively, this behavior is what our and other research groups have observed also in the case of a  $CH_4$ -CPO experiment on rhodium, and can be fully explained by the catalytic production of syngas on rhodium.<sup>[4,9–11]</sup> Thus, integral measurements (i.e., measurements of temperature and composition collected exclusively at the reactor outlet) would have suggested the unique existence of a heterogeneous process. A purely catalytic process was, for instance,

[\*] Dr. A. Donazzi, D. Livio, Dr. M. Maestri, Prof. A. Beretta, Prof. G. Groppi, Prof. E. Tronconi, Prof. P. Forzatti  
Laboratory of Catalysis and Catalytic Processes  
Dipartimento di Energia, Politecnico di Milano  
Piazza Leonardo da Vinci 32, 20133 Milano (Italy)  
Fax: (+39) 0223993284  
E-mail: alessandra.beretta@polimi.it  
Homepage: <http://www.lccp.polimi.it>

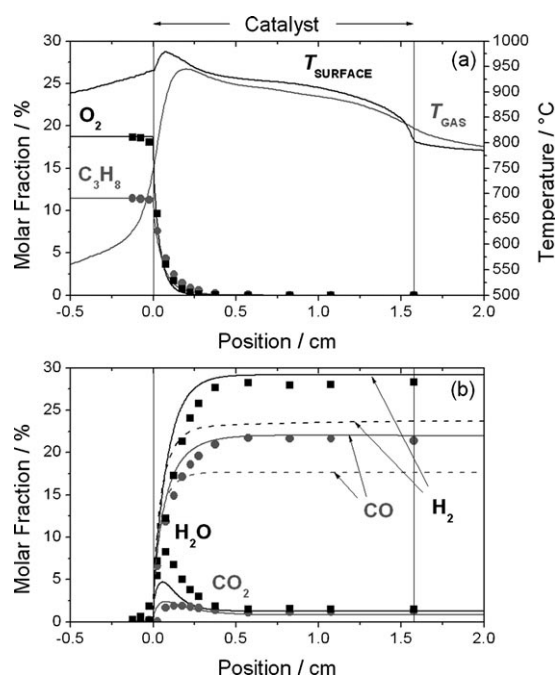


**Figure 1.** Spatially resolved profiles of temperature and composition for a  $C_3H_8$  CPO experiment. a) Reactants and temperature. b) Products. 2 wt% Rh/ $\alpha$ - $Al_2O_3$  catalyst supported over a 400 cpsi cordierite honeycomb. Flow rate =  $5\text{ L min}^{-1}$  (STP),  $P = 1\text{ atm}$ . Feed:  $C_3H_8$ /air,  $C_3H_8 = 11\text{ vol\%}$ ,  $O/C = 1.12$ . Experimental results (symbols) and calculations according to the kinetic model (lines; see text for details) are reported. The temperature profiles are experimental measurements. Dashed lines are calculations obtained by neglecting the steam reforming reactions of  $C_2H_6$ ,  $C_2H_4$ , and  $C_3H_6$  in the heterogeneous kinetic scheme. cpsi = cells per square inch.

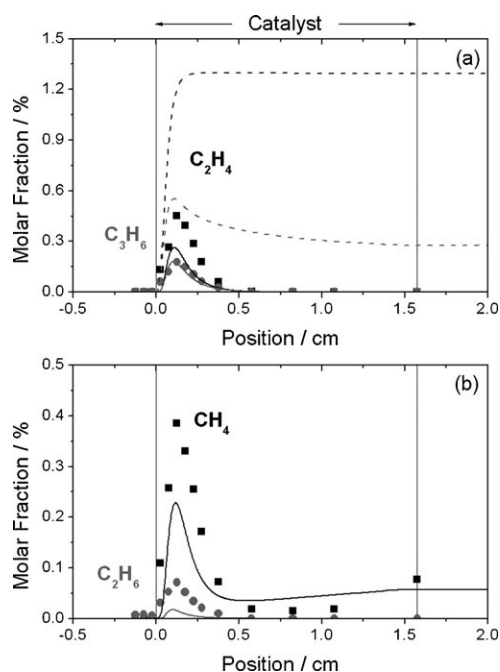


**Figure 2.** Spatially resolved composition profiles in a  $C_3H_8$  CPO experiment. a) Unsaturated by-products. b) Saturated by-products. Conditions, lines, and symbols as in Figure 1.

inferred by Deutschmann and co-workers,<sup>[12]</sup> who analyzed integral data of iso-octane partial oxidation over Rh at  $O/C > 1$ . However, the spatially resolved measurements described herein reveal for the first time that several other species, such as  $C_2H_4$ ,  $C_3H_6$ , and  $C_2H_6$ , were formed at the reactor inlet, passed through concentration maxima, and were then completely consumed before the ending section of the catalyst (Figure 2).

We also observed a complex evolution of  $CH_4$  that, similarly to  $C_2$  and  $C_3$  species, was initially formed and then consumed within the first half of the reactor, but tended to be formed again in the ending portion of the reactor. On the one hand, since the formation of hydrocarbon species such as olefins cannot be explained by the syngas formation pathways on rhodium, this experimental finding provided evidence of gas-phase chemistry. On the other hand, the gas-phase chemistry alone could not explain the outlet-selective formation of syngas. Hence, a possible scenario could be that the intermediates generated in the gas phase adsorbed back onto the catalyst surface and eventually converted to syngas.

To help the interpretation of the experiments, a heterogeneous 1D mathematical model of the adiabatic honeycomb monolith was applied, which fully describes mass and heat transfer phenomena in the solid and gas phases.<sup>[9,13]</sup> Detailed gas-phase chemistry was taken from Ranzi et al.<sup>[14]</sup> Concerning the surface chemistry, we incorporated a kinetic model of the partial oxidation of  $C_3H_8$  to syngas on rhodium, independently derived by a dedicated kinetic study in an isothermal microreactor. The model accounts for the formation of syngas through a consecutive scheme, consisting of deep oxidation and steam reforming of propane and methane, water-gas shift,  $H_2$  and  $CO$  post-combustion, and methanation. The propane scheme was also extended to account for the catalytic conversion of hydrocarbon intermediates generated in the gas phase, such as  $C_2H_6$ ,  $C_2H_4$ , and  $C_3H_6$ . All the general trends of product distribution were captured by the model (solid lines in Figure 1 and Figure 2). This result is very satisfactory, considering that the simulations were fully predictive and no parameter was adjusted to match the data. The model analysis revealed that gas-phase activation of  $C_3H_8$  was responsible for the production of all the hydrocarbon species observed at the reactor inlet: cracking and dehydrogenation reactions can explain the formation of  $CH_4$ ,  $C_2H_4$ , and  $C_3H_6$ . According to the model, the consumption of  $O_2$  was almost entirely due to surface oxidation reactions (mass-transfer controlled), while homogenous oxidative pyrolysis played a negligible role. Formed in the gas phase, the hydrocarbon species were then mainly consumed on the catalytic surface by steam reforming with formation of syngas. The consecutive reactions of these species are in fact much slower in the gas phase than on the rhodium surface.

Concerning the complex evolution of  $CH_4$ , the simulations showed that this experimental result could be very well explained by a series of contributions consisting of 1) gas-phase formation of methane by propane cracking, 2) its catalytic consumption by steam reforming, and 3) its catalytic formation by methanation (kinetically favored by the increasing partial pressures of  $H_2$  and  $CO$  and thermodynamically favored by the decreasing temperatures).

By conducting simulations in which the heterogeneous conversion of hydrocarbon intermediates generated in the gas phase is neglected, we verified that the evolutions of temperature and product distribution are not correctly described in this case (dashed lines in Figure 1 and Figure 2). The overall production of  $H_2$  and CO would be greatly underestimated (Figure 1b), while the outlet composition would be rich in olefins and other hydrocarbons (Figure 2a). Moreover, predicted outlet temperatures would be much higher than observed (Figure 3).

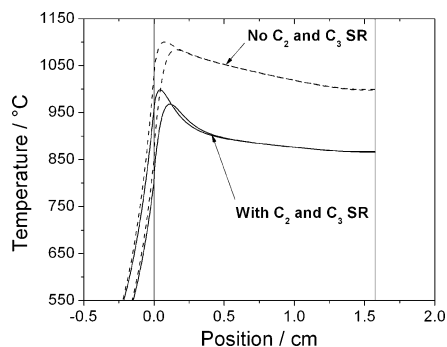


**Figure 3.** Calculated temperature profiles for the gas phase and the solid surface in a  $C_3H_8$  CPO experiment. Conditions as in Figure 1. SR = steam reforming.

Thus, in spite of the very high catalytic activity of rhodium in the production of syngas, this experiment showed for the first time that the conversion of propane to syngas also includes a “by-pass” route in the gas phase, which involves the conversion of propane to smaller, reactive hydrocarbon species and their consecutive heterogeneous conversion to syngas. This finding is a clear indication of a concerted heterogeneous–homogeneous process. Under the operating conditions of interest for the small-scale production of  $H_2$  studied herein, this interaction turns out to be a synergy: gas-phase reactions enrich the main fuel with additional reactive species that make the catalytic conversion to syngas even faster and more efficient. Nevertheless, undesired consequences can be also envisaged, such as loss of selectivity, soot formation, and catalyst deactivation if the by-pass line breaks and gas-phase intermediates do not complete their catalytic conversion to syngas (at higher temperatures, for instance). All these aspects have a crucial impact and must be taken into account for the design and safe operation of distributed hydrogen units.

The new mechanistic picture that we draw from this case can be easily generalized and fully explains all the results in the literature. Specifically, the by-pass route is significant only when the thermal activation of C–H bonds is sufficiently fast, which rules out the case of methane activation at atmospheric pressure and explains why methane CPO is mainly a heterogeneous process. Also, the by-pass may exist only if the reforming capability of the catalyst is sufficiently high to quench the gas-phase chain process; this condition becomes critical for platinum, which has much lower reforming activity

than rhodium, and explains why the ODH of short alkanes on platinum is mainly a homogeneous process.

Understanding of this concerted mechanism was made possible by the application of the in situ sampling technique coupled with detailed modeling of gas-phase and surface kinetics. This powerful combination of methodologies has revealed the complex harmony with which surface and gas-phase reactions cooperate in the high-temperature short-contact-time partial oxidation of hydrocarbons.

## Experimental Section

The catalyst (2 wt % Rh/ $\alpha-Al_2O_3$ ) was prepared by incipient wetness impregnation of  $\alpha-Al_2O_3$  powders with an aqueous  $Rh(NO_3)_3$  solution and then supported over a 400 cpsi cordierite honeycomb monolith (16 mm long, 23 mm diameter). The final catalyst loading amounted to 720 mg. The  $C_3H_8$  CPO experiments were performed at atmospheric pressure by feeding  $C_3H_8$ /air mixtures ( $O/C = 1.12$ ,  $C_3H_8 = 11$  vol %) at  $5\text{ L min}^{-1}$  (STP) flow rate. The reactor consisted of an externally insulated stainless steel tube with a quartz liner to prevent formation of coke. The catalytic honeycomb was placed in between two inert heat shields (a FeCrAlloy foam and a 400 cpsi honeycomb) kept 1.5 cm from the inlet and the outlet section of the catalyst.

For the spatially resolved temperature measurements, the reactor was equipped with a K-type thermocouple (0.25 mm diameter) and with a narrow-band infrared pyrometer (Impac Infrared, IGA 5-LO) connected to an optical fiber (Polymicro, FVP300, 1.5 m long). The IR detector of the pyrometer was an indium–gallium–arsenic photodiode sensitive to radiation in the wavelength range 1.45–1.8  $\mu\text{m}$  and calibrated between 350 and 1100 °C. The optical fiber (300  $\mu\text{m}$  core diameter, 330  $\mu\text{m}$  OD, 45° cut tip) was housed inside a transparent quartz capillary (530  $\mu\text{m}$  ID, 670  $\mu\text{m}$  OD) sealed at one end, which acted as an inert sleeve for the fiber and was moved by a linear translation stage. It is important to note that the signal of the pyrometer is affected by artifacts at the boundary of the monolith (e.g. the measurement of high temperatures before the catalytic monolith and the sudden drop of temperature close to the exit monolith section),<sup>[9]</sup> owing to the fact that the optical fiber tip tends to collect some light also from zones in front of it. These phenomena do not significantly influence the temperature measurement within the monolith channel.

For the spatially resolved gas-phase composition measurements, the sampling system consisted of a quartz capillary (200  $\mu\text{m}$  ID, 340  $\mu\text{m}$  OD) inserted into the central channel of the honeycomb. The capillary was cut at one end and connected to the linear actuator at the other end. The gases were sampled at specific axial positions and pumped to a micro gas chromatograph (3000 A, Agilent Technologies) through the capillary. The sampling flow ( $5\text{ cm}^3\text{ min}^{-1}$  (STP)) did not alter the reacting flow of the single monolith channel.

Received: November 22, 2010

Revised: December 31, 2010

Published online: March 22, 2011

**Keywords:** catalytic partial oxidation · gas-phase reactions · heterogeneous catalysis · high-temperature chemistry · hydrocarbons

[1] T. V. Choudhary, V. R. Choudhary, *Angew. Chem.* **2008**, *120*, 1852–1872; *Angew. Chem. Int. Ed.* **2008**, *47*, 1828–1847.

[2] A. S. Bodke, D. A. Olschki, L. D. Schmidt, E. Ranzi, *Science* **1999**, *285*, 712–715.

[3] D. A. Goetsch, L. D. Schmidt, *Science* **1996**, *271*, 1560–1562.

- [4] R. Horn, K. A. Williams, N. J. Degenstein, A. Bitsch-Larsen, D. D. Nogare, S. A. Tupy, L. D. Schmidt, *J. Catal.* **2007**, *249*, 380–393.
  - [5] R. Horn, K. A. Williams, N. J. Degenstein, L. D. Schmidt, *J. Catal.* **2006**, *242*, 92–102.
  - [6] R. Schwiedernoch, S. Tischer, C. Correa, O. Deutschmann, *Chem. Eng. Sci.* **2003**, *58*, 633–642.
  - [7] J. P. Lange, R. J. Schoonebeek, P. D. L. Mercera, F. W. van Breukelen, *Appl. Catal. A* **2005**, *283*, 243–253.
  - [8] B. C. Michael, D. N. Nare, L. D. Schmidt, *Chem. Eng. Sci.* **2010**, *65*, 3893–3902.
  - [9] A. Donazzi, M. Maestri, B. C. Michael, A. Beretta, P. Forzatti, G. Groppi, E. Tronconi, L. D. Schmidt, D. G. Vlachos, *J. Catal.* **2010**, *275*, 270–279.
  - [10] A. Donazzi, B. C. Michael, L. D. Schmidt, *J. Catal.* **2008**, *260*, 270–275.
  - [11] R. Horn, N. J. Degenstein, K. A. Williams, L. D. Schmidt, *Catal. Lett.* **2006**, *110*, 169–178.
  - [12] M. Hartmann, L. Maier, H. D. Minh, O. Deutschmann, *Combust. Flame* **2010**, *157*, 1771–1782.
  - [13] M. Maestri, A. Beretta, G. Groppi, E. Tronconi, P. Forzatti, *Catal. Today* **2005**, *105*, 709–717.
  - [14] E. Ranzi, A. Sogaro, P. Gaffuri, G. Pennati, T. Faravelli, *Combust. Sci. Technol.* **1994**, *96*, 279–325.
-